A&A 448, 221–229 (2006)
DOI: 10.1051/0004-6361:20052653
© ESO 2006

Astronomy & Astrophysics

A search for fine structure inside high resolution profiles of weak diffuse interstellar bands⋆

K. Słyk[1], G. A. Galazutdinov[4,2], F. A. Musaev[1,2], A. V. Bondar[5], M. R. Schmidt[3], and J. Krełowski[1]

[1] Center for Astronomy, Nicholas Copernicus University, Gagarina 11, 87-100 Toruń, Poland
e-mail: [kasiek;jacek]@astri.uni.torun.pl
[2] Special Astrophysical Observatory, Nizhnij Arkhyz 369167, Russia
e-mail: faig@sao.ru
[3] N.Copernicus Astronomical Center, Rabiańska 8, 87-100 Toruń, Poland
e-mail: schmidt@ncac.torun.pl
[4] Korean Astronomy Observatory, Optical Astronomy Division, 61-1, Whaam-Dong, Yuseong-Gu, Daejon, 305-348, Korea
e-mail: gala@boao.re.kr
[5] International Centre for Astronomical, Medical and Ecological Research (IC AMER), Terskol, 361605, Russia
e-mail: arctur@terskol.com

Received 7 January 2005 / Accepted 4 October 2005

ABSTRACT

This paper presents a survey of the high-resolution profiles of selected, moderately weak diffuse interstellar bands (DIBs) between 4725 and 6730 Å. In very high signal-to-noise spectra, obtained as a result of averaging several individual exposures of reddened, early-type stars that show Doppler splitting of <2 km s^{-1} in interstellar gas lines, the profiles seem to have a substructure. This supports the molecular origin hypothesis for DIBs. We studied the profiles of the diffuse interstellar bands at wavelengths of 4726.33, 4963.85, 5418.89, 5541.74, 5544.95, 5546.46, 5762.73, 5766.05, 5769.09, 6439.41, 6445.53, 6449.16, 6729.28 Å.

Key words. ISM: clouds – ISM: molecules

1. Introduction

Diffuse interstellar bands (DIBs) were first mentioned as stationary features in spectroscopic binaries more than 80 years ago by Heger (1921). Merrill et al. (1937) argued they were interstellar in nature. At the beginning, when they were being observed in photographically recorded spectra of heavily reddened stars, the list of known features grew rather slowly. Its rapid growth started after broad application of solid-state receivers about 20 years ago. The number of known features has arisen to almost 300 (Galazutdinov et al. 2000), as a result of increasing resolution and signal-to-noise (*S/N*) ratios of the spectra currently being acquired. Despite many efforts, determining the physical cause of DIBs remains the longest standing unsolved problem in all of spectroscopy. The physical cause facilitating the formation and/or preservation of the DIB carriers is unknown, although the conditions can potentially be deduced from some analysis of interstellar spectral features of well-known atoms or molecules.

While trying to identify DIB carriers one can analyse:

- mutual relations between pairs of DIBs in order to compose sets possibly originated by the same species
- correlations between DIB strengths and those of atomic interstellar lines
- correlations between DIB strengths and the features of simple interstellar molecules such as CH, CN, CO, H_2, etc.
- details of DIB profiles that are very likely to be specific to possible carriers like those found in laboratory spectra of complex molecules.

The first analysis of profiles was made by Herbig (1975), who added 24 new DIBs to the existing list using computer-averaged spectra of many heavily reddened stars. Among 39 then known DIBs, he was able to distinguish some features with non-symmetrical profiles; some very striking differences between the widths of such DIBs as 4430 and 6196 were demonstrated as well. One phenomenon that presumably modifies DIB profiles in reddened stars is Doppler splitting of the IS components, through this is seldom seen because of the diffuseness of the DIBs (but see Herbig & Soderblom 1982). To obtain intrinsic profiles of diffuse interstellar bands, one must observe spectra of slightly reddened early-type stars where

⋆ Based on data collected at the Terskol 2 m telescope operated at the IC AMER Observatory, Russia.

Article published by EDP Sciences and available at http://www.edpsciences.org/aa or http://dx.doi.org/10.1051/0004-6361:20052653

Table 1. The list of observed stars. Column headings represent: HD – HD number; Name; Sp/L – spectral and luminosity class; V – visual apparent magnitude; $E(B-V)$ – colour excess; $T_{\rm eff}$ – effective temperature; $\log g$ – gravity; $v \sin i$ – rotational velocity.

HD	Name	Sp/L	V	$E(B-V)$	$T_{\rm eff}$	$\log g$	$v \sin i$
23180	o Per	B1 III	3.86	0.29	23 200	3.00	85
24398	ζ Per	B1 I	2.88	0.34	23 000	2.73	59
148184	χ Oph	B2 IVpe	4.42	0.44	20 000	4.00	134
149757	ζ Oph	O9.5 V	2.58	0.30	35 900	3.94	379
179406	20 Aql	B3 V	5.33	0.30	18 000	4.00	170

interstellar gas lines show only small Doppler effects. Such work was started by Krełowski & Walker (1987) and by Westerlund & Krełowski (1988), soon after application of solid state detectors in astrophysics. They proved that diffuse features have non-Gaussian profiles and suggested a presence of some substructures inside them. At that time, such an analysis was only possible in cases of strong features, such as 5797 and 6379, because of the still limited resolution and signal-to-noise ratio.

The spectra with the highest resolution, acquired with the Ultra High Resolution Facility (R = 600 000), demonstrated a similarity between the 5797 and 6614 DIB profiles (Sarre et al. 1995; Kerr et al. 1998). The latter seem to contain substructures that could be P, R, and Q branches of the rotational contours for the bands of some complex molecules. Schulz et al. (2000) then showed that calculated profiles of some partially hydrogenated carbon chains are very similar to the intrinsic profile of 6614. This similarity suggests that diffuse interstellar bands are likely to originate in large, carbon-based molecules. The most promising carrier candidates are polycyclic aromatic hydrocarbons (PAHs – see e.g. Salama et al. 1999; Ruiterkamp et al. 2002), linear (hydro)carbon molecules (see e.g. Motylewski et al. 2000), and fullerenes (see e.g. Foing & Ehrenfreund 1995).

The survey conducted by Krełowski & Schmidt (1997) based on R = 60 000 spectra showed that some substructures seem to be intrinsic to almost all narrow DIBs profiles. In broad features, no substructures have been found. This phenomenon was clearly demonstrated in the case of very broad 4430 diffuse interstellar band by Snow (2002). However, a study of broad DIBs is difficult because their shapes as extracted from echelle spectra are very uncertain, so detailed studies of DIB profiles concern rather narrow features. As shown recently (Galazutdinov et al. 2002a), the profile details, observed inside strong diffuse interstellar bands, can differ from one line of sight to another. The profiles do not change in unison, even when their intensities are very well-correlated (for 6196 and 6614).

A vast majority of diffuse interstellar bands are weak features (Galazutdinov et al. 2000) with a central depth that does not exceed 1% of the continuum level, which is why the high *S/N* ratio spectra are necessary to search for their fine structure. The first work that analysed the high resolution and *S/N* profiles of weak DIBs showed the presence of substructures inside them (Galazutdinov et al. 2002b). Some patterns of DIB profiles may also be blends of single features from different carriers. Nevertheless, the similarity of high resolution profiles of certain DIBs may be an additional argument to support the hypothesis of their common origin.

Until now, the substructures have been detected only inside profiles of very few weak DIBs. It thus seems important to search for profile details inside as many as possible of the weak diffuse interstellar bands, which will open the way to detailed studies of the similarities between the profiles of strong and weak features. It seems likely (if all DIBs are originated by some complex molecules) that substructures should be intrinsic to almost all profiles.

The existing analyses prove that a search for DIB substructures requires a resolution $R > 100\,000$. Lower resolutions, like that applied by Krełowski & Schmidt (1997), only allow one to suggest the presence of some fine structure inside a profile. A sufficiently high resolution instead allows one to distinguish between the profiles of interstellar lines and those of stellar or telluric contaminating features. Although this paper concerns only these DIBs, which are situated in regions where there is no heavy telluric contamination, a proper identification of stellar features seems to be of basic importance. It requires, however, not only proper resolution but also precise modelling of stellar spectra.

2. Observational data

The spectra analysed in this project were acquired using the coudé echelle spectrometer (Musaev et al. 1999) fed by the 2 m telescope of the Observatory on the Peak Terskol (Northern Caucasus). The detector is a Wright Instruments CCD 1242 × 1152 matrix camera (pixel size 22.5 μm × 22.5 μm). With a resolving power of R = 120 000, the range ~3500 Å–~10 100 Å is covered in three exposures. We reduced each spectrum using the DECH code (Galazutdinov 1992), which provides all stages of CCD echelle-image-spectra processing: flatfield division, bias/background subtraction, one-dimensional spectrum extraction from the 2-dimensional images, correction for the diffuse light, spectrum addition and excision of cosmic ray features. The DECH code also allows location of a fiducial continuum, and measurements of the line equivalent widths, line positions and shifts.

The wavelength scale was done according to a wavelength calibration standard spectrum (Th+Ar hollow–cathode lamp or to any bright radial velocity standard star e.g. Procyon or the Solar spectrum). DIB positions were determined on the basis of a survey done by Galazutdinov et al. (2000).

Table 1 contains characteristics of target stars, i.e. their HD numbers, names, spectral types, luminosity classes, magnitudes, colour excesses, effective temperatures, surface

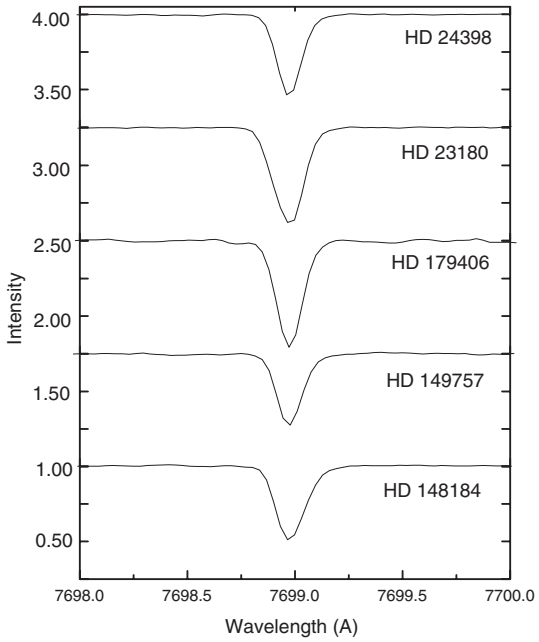

Fig. 1. Profiles of the interstellar KI lines in the $R = 120\,000$ spectra of all target objects.

gravities, and rotational velocities. The stars were chosen because of small Doppler splitting in CH (4300.31 Å) and KI (7698.96 Å). In Fig. 1, the profiles of KI line in the spectra of target stars are plotted. In this line, Doppler splitting is not detectable at the resolution $R = 120\,000$. Higher resolution spectra by Welty & Hobbs (2001) show multiple components in all of our stars except HD 179406. The lack of KI splitting in our spectra allows the assumption that DIBs are not modified by this effect. The lines of KI and CH show a tight correlation with some strong DIBs (Krełowski et al. 1998, 1999), which suggests a spatial correlation of some DIB carriers with these species. It seems likely that the carriers of weak and narrow DIBs, apparently related to those considered in the above papers, are also spatially related to KI and CH. This fact could be, additionally, confirmed by correlation of some moderately weak DIBs with CH as shown by Thorburn et al. (2003).

As telluric line divisors, we used two rapidly rotating, non-reddened B stars: HD 120315 and HD 218045. The interstellar atomic and molecular lines allowed us precisely to determine radial velocities of the intervening interstellar clouds during any single observation. Every spectrum was shifted to the rest-wavelength velocity frame of interstellar features.

High resolution of echelle spectra causes rows of spectra to be wider than the size of CCD matrix; thus, each spectrum contains only about one third of the full wavelength range mentioned above. Covering the full waverange is possible using three partially overlapping settings of the spectrograph: e.g. the range 4700–4750 Å is covered in three spectra; the rows contain the ranges 4699.38–4723.92 Å (the spectrum with the setting "a" of the spectrograph), 4715.80–4737.56 Å (setting "b"), and 4723.31–4750.98 Å (setting "c"); DIB at the wevelength of 4726.33 Å is visible in spectra with setting "b" and "c" of the spectrograph. Table 2 presents the log of observations, which contains: date of observation, the setting of the spectrograph (letters: a, b, c), HD numbers of stars recorded during the night, and DIBs visible in the spectra recorded with the setting. The cover of the wavelength range implies the number of spectra that were used in the averages to produce detailed DIB profiles. The features that were situated close to the edges of the echelle spectra were neglected because of low *S/N* and of uncertain continuum levels. Our considerations were restricted to relatively narrow DIBs, so that the profiles of selected features are free of heavy telluric contamination.

Table 2. The log of observations. Column headings represent: UT Date – date of observation, Star – HD numbers of targets recorded during the night, DIB – DIBs visible in the setting of the spectrograph. Letters a, b, c represent the spectrograph setting (see the text).

UT Date	Star	DIB
Aug. 26, 2001 c	23180	4726.33, 5418.89,
Aug. 27, 2001 c	24398, 23180	5762.73, 5766.05,
Aug. 28, 2001 c	24398, 23180	5769.09, 6729.28
Aug. 29, 2001 c	24398, 23180	
Oct. 22, 2001 c	23180	
Oct. 23, 2001 c	24398	
Oct. 25, 2001 c	24398, 23180	
Oct. 26, 2001 c	24398, 23180	
Oct. 28, 2001 c	24398, 23180	
Jan. 18, 2002 a	24398, 23180	4963.85, 5418.89,
Jan. 22, 2002 a	23180	5541.74, 5544.95,
Jan. 23, 2002 a	148184, 149757	5546.46, 6439.41,
Jan. 24, 2002 a	24398, 23180	6445.53, 6449.16
Jan. 28, 2002 a	23180	
May 22, 2004 b	148184, 149757	4726.33, 5762.73,
May 23, 2004 b	148184, 149757	5766.05, 5769.09
May 24, 2004 b	148184, 149757	
Aug. 22, 2004 b	24398, 23180, 179406	
Aug. 26, 2004 b	24398, 23180	
Aug. 27, 2004 b	179406	

3. Results

To test the method, we compared the well–known profile of 6614 in an average spectrum with the same profile presented by Walker et al. (2000). This comparison is shown in Fig. 2. The first profile was taken with the Gecko spectrograph on the 3.6 m Canada-France-Hawaii Telescope ($R = 120\,000$), and the averaged Terskol profile was obtained from 5 spectra of the same star – HD 23180 ($R = 120\,000$). It is evident that in both cases the profile shows the same internal structure.

The contamination by stellar lines must be carefully checked to make a proper extraction of the shape of DIB profiles possible from the observed spectra. It is particularly important in cases of slow rotators, and it depends on the relative strength of DIBs and stellar lines. The identification of potentially important stellar lines was made by means of spectral synthesis. The synthetic spectrum was calculated around each DIB and for all stars from Table 1. We did not try to build individual non-LTE atmospheric models, but instead chose the atmospheric models from Kurucz's grid (Kurucz 1992, 1993a) with the temperatures, gravities, and rotational velocities given in Table 1. For some objects, published atmospheric parameters

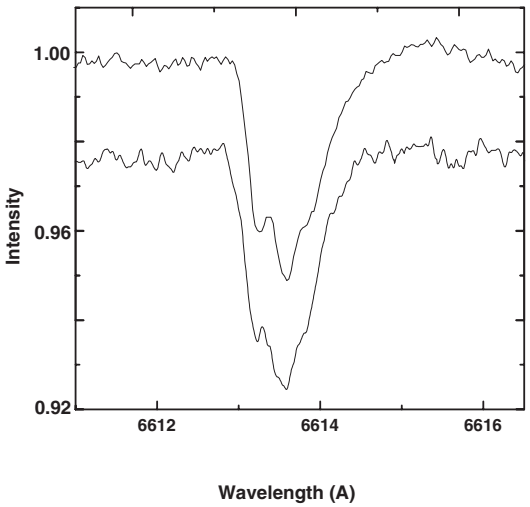

Fig. 2. Comparison of the profiles of the DIB 6614 in the spectra of o Per acquired with the aid of both the Gecko spectrograph, R = 120 000, fed with the 3.6 m Canada-France-Hawaii Telescope (Walker et al. 2000) (*top*) and the coudé echelle spectrometer, R = 120 000, (Musaev et al. 1999) fed with the 2 m Terskol telescope (*bottom*).

were used: HD 23180, Lyubimkow (1998); HD 24398, McErlean et al. (1999); HD 149757, Lamers & Leitherer (1993). For the remaining two objects, effective temperatures were based on the calibration of Underhill et al. (1979), and gravity was fixed to $\log g = 4.0$. We believe that such a crude procedure is sufficient for our purpose. As an input list of lines, we used the VALD database (Piskunov et al. 1995). The origin of the atomic data of lines identified in any of the spectral windows was Kurucz's database (Kurucz 1993b). In addition, the atomic data of lines were verified by comparison with NIST Atomic Spectra Database (Martin et al. 1999), where available. If there exist in our targets some features absent in synthetic spectra, which are comparable in strength to the substructures in weak DIBs, the rotation of the stars would broaden and flatten them, so that such structures would be hardly distinguishable from the continnum.

A special procedure was applied in the case of absorption lines of CII apparently contaminating the 4726.33 and 4963.85 DIBs (see also Galazutdinov et al. 2001) and not available in the NIST database. We used the spectrum of γPeg (HD 886, B2IV) to determine their oscillator strengths, while an upper limit was determined in some cases. Atomic abundances and stellar parameters were taken from Gies & Lambert (1992) ($v \sin i = 6$, $T_{\rm eff} = 22\,670$ K, $\log g = 4.02$). This procedure was extended to all lines belonging to the same multiplet, where available. The atomic lines used in the synthesis of the spectra within 3 Å of the positions of the potentially contaminated DIBs are listed in Table 3. The potential effect of contaminations may be checked by comparison with equivalent widths of the lines we studied, as measured in the spectrum of γPeg – see Col. 6 of Table 3.

As seen in Table 3, we relied only on the laboratory oscillator strengths given in the NIST database or on semiempirically determined values of $\log gf$, if the laboratory data were not available. Thus, some differences appear in the lists

Table 3. The list of stellar atomic lines contaminating the selected DIBs. Column headings represent: DIB; Wavelength [Å] – of stellar line; Ion – line identification; *EP* [eV] – excitation potential; $\log gf$ – oscillator strength; *EW* [mÅ] – equivalent width measured in γPeg; Source – reference.

DIB	Wavelength	Ion	*EP*	$\log gf$	*EW*	Source
4726.33						
	4726.868	ArII	17.14	–0.103	6.2	NIST
	4727.410	CII	24.79	–0.730[a]	<2	Heb83
	4730.521	SiIII	28.79	–0.281	<3	NIST
4963.85						
	4964.736	CII	22.57	–0.700[a]	6.6	Bell
	4965.079	ArII	17.26	–0.234	6.7	NIST
5541.74, 5544.95, 5546.46						
	5539.926	SiIII	28.12	–0.359	<2	NIST
	5540.061	NII	25.49	–0.557	<2	NIST
	5543.471	NII	25.50	–0.092	<2	NIST
5762.73, 5766.05, 5769.09						
	5764.419	NeI	18.55	–0.370[a]	3.7	Bell
	5767.450	NII	18.50	–1.437	6.1	NIST
6139.94						
	6136.890	NII	23.13	–1.124	<2	NIST
	6143.063	NeI	16.62	–0.098	3.8	NIST
6729.28						
	6727.070	CII	22.53	–1.065	12.8[b]	NIST
	6727.260	CII	22.53	–0.919		NIST
	6727.480	CIII	38.21	–0.642		NIST
	6731.040	CIII	38.22	–0.293	6.8	NIST

NIST – Martin et al. (1999).
Heb83 – Heber (1983).
Bell light – Kurucz & Bell (1995).
[a] Semi-empirical $\log gf$.
[b] *EW* of 3 unseparated lines.

of contaminating stellar lines in comparison with an earlier work (Galazutdinov et al. 2001), especially visible around the 4726.33 DIB.

All calculations were done using Hubeny's SYNSPEC code (Hubeny et al. 1986, 1995). The solar composition was assumed, and the microturbulence arbitrarily set to 5 km s^{-1}. The rotational velocities were adopted from Table 1.

According to the rotational velocities of the target stars, the stellar contaminations are most important in HD 23180 and HD 24398, which are slow rotators. In the remaining objects, the rotation reduces the contaminating effect of weak stellar lines significantly. Additionally, all the spectra were shifted so as to bring the interstellar features to their rest wavelengths. The amount of such a shift depends on the radial velocity of the interstellar cloud, and it is different for each line of sight. Thus the position of stellar lines differs in every spectrum, while in the average spectra their influence lessens. Figure 3 shows the range between 4680 and 4740 Å in HD 23180. This range contains the weak 4726.33 DIB. The figure clearly shows that the synthetic spectrum allows identification of every stellar feature. The calculated spectrum also demonstrates

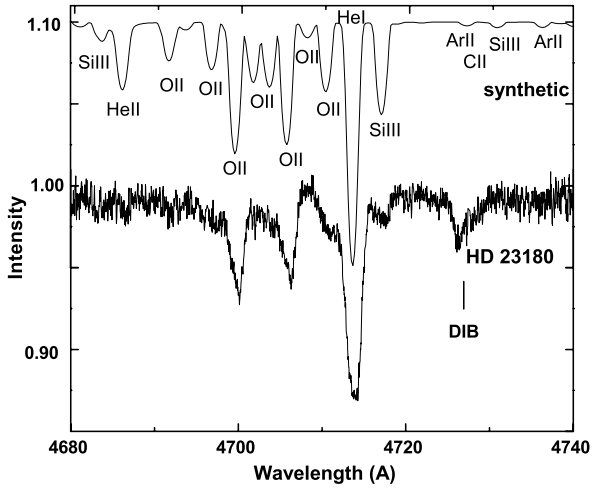

Fig. 3. The spectrum of HD 23180 (in the vicinity of the 4726.33 DIB) compared to the synthetic one. Note the minor possibility of contamination of the DIB profile.

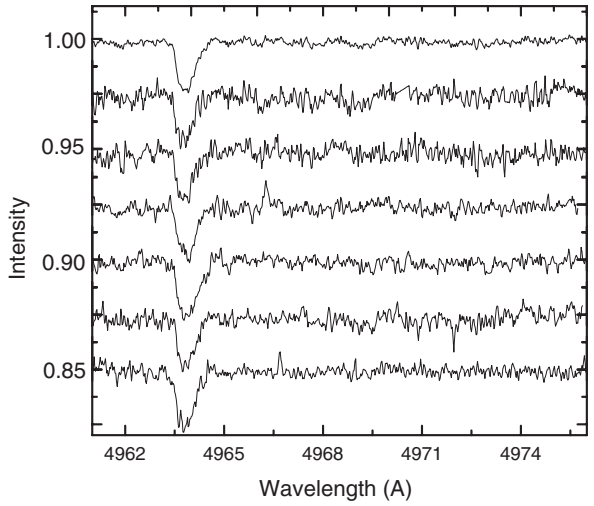

Fig. 4. Six individual spectra of HD 23180 and the resulting spectrum (*top*) in the vicinity of the 4964.85 DIB. Note the reduction in noise when the mean stellar spectra are coadded.

features that are below the threshold of detection in *o*Per spectrum. In the vicinity of the DIB one can notice profile the weak ArII 4726.851 Å, CII 4727.410 Å, and SiIII 4730.521 Å stellar lines. However, the influence of these features can be neglected, as even stronger lines are barely traced in the HD 23180 spectrum. The 4726.33 diffuse band is presented in detail in Fig. 5.

The procedure of coadding spectra increases the net *S/N*. Figure 4 shows six individual exposures of HD 23180 ($S/N \sim$ 300–~500) and the resulting spectrum ($S/N \sim 800$) in the range containing 4964.85 DIB. It is clearly seen there that structures caused by noise in single spectra both within and outside the band decreate and do not produce any artificial features in the average spectrum. Only gross, common features of the profiles are retained, so that individual star differences are averaged out. Especially in the case of *o*Per, which is a spectroscopic binary, Doppler effect moves stellar lines back and force in relation to stationary interstellar features.

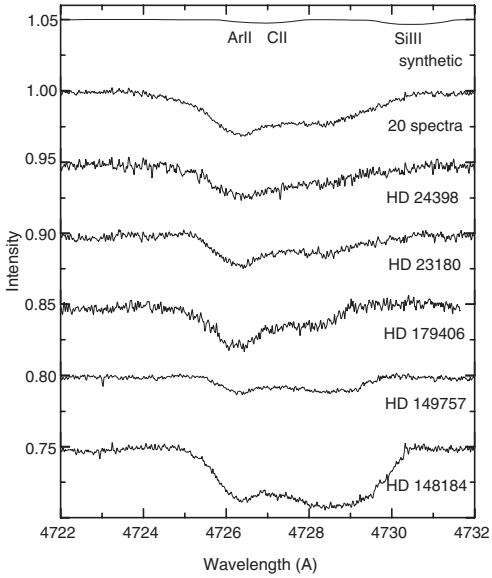

Fig. 5. The detailed profile of the 4726.33 diffuse band. The synthetic spectrum allows weak ArII 4726.851 Å, CII 4727.410 Å, and SiIII 4730.521 Å stellar lines to be identified.

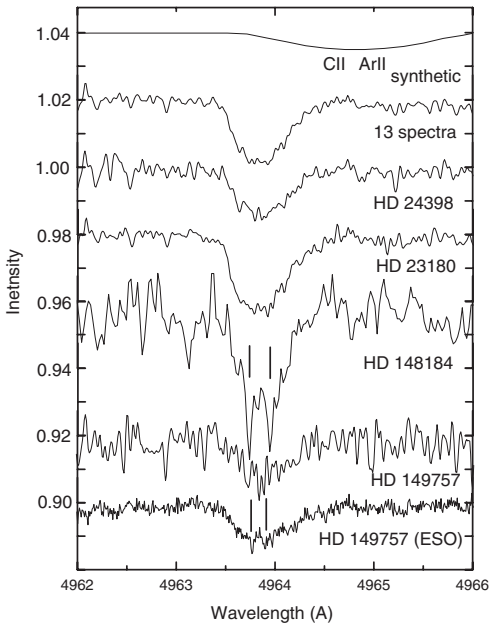

Fig. 6. Profile of the 4963.85 DIB observed towards HD 24398, HD 23180, HD 148184, and HD 149757 compared to the general average of 13 spectra and the ESO (R = 220 000) spectrum of HD 149757 (the substructures marked with vertical lines). The synthetic spectrum (above) shows the blend of possibly contaminating CII 4964.736 Å and ArII 4965.079 Å stellar lines.

Figures 5–11 present the profiles of weak DIBs: the average of all available spectra and also averages of spectra for the individual stars. The synthetic spectra of slightly different types of target stars show the same set of stellar lines, so the figures contain only one synthetic spectrum ($T_{\rm eff}$ = 23 000 K, $\log g$ = 3.0, $v \sin i$ = 60). This calculated spectrum shows the strongest potential contamination of the derived DIB profiles. In the case of other targets the rotation lessens the influence of stellar lines. Tables 3–9 contain measurements of equivalent

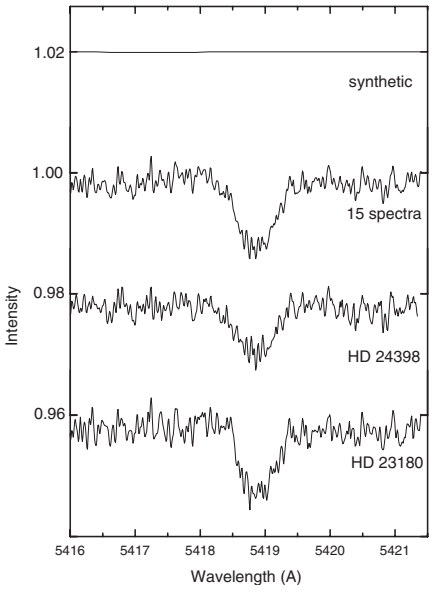

Fig. 7. The general average profile of the 5418.89 DIB compared with two individual ones. Stellar lines are absent in its vicinity.

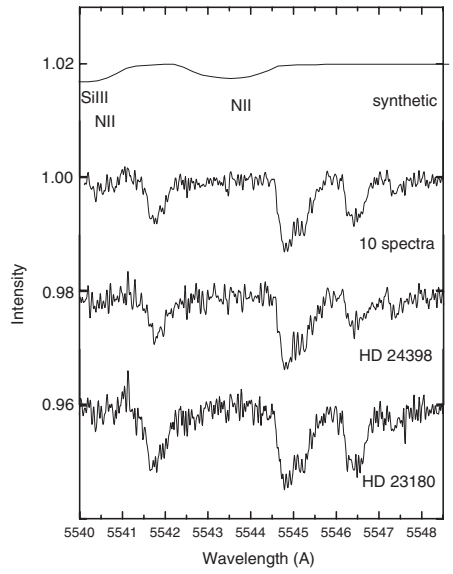

Fig. 8. The profiles of 5541.74, 5544.95, and 5546.46 DIBs. The synthetic spectrum shows SiIII 5539.926 Å, NII 5540.061 Å, and NII 5543.471 Å possibly contaminating stellar lines in this wavelength range.

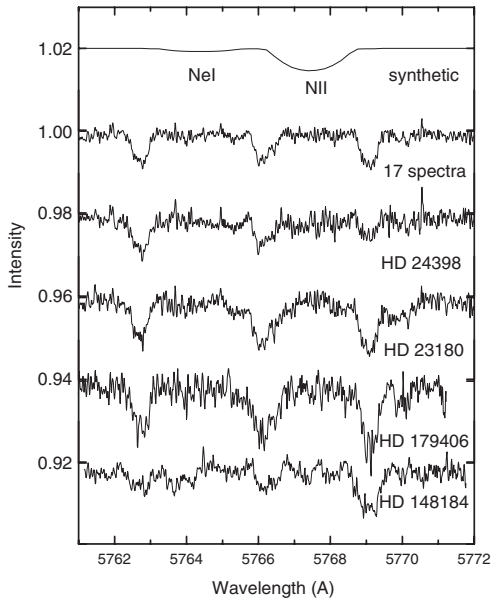

Fig. 9. The profiles of 5762.73, 5766.05, and 5769.09 DIBs. The synthetic spectrum identifies two possibly contaminating lines: NeI 5764.419 Å and NII 5767.446 Å.

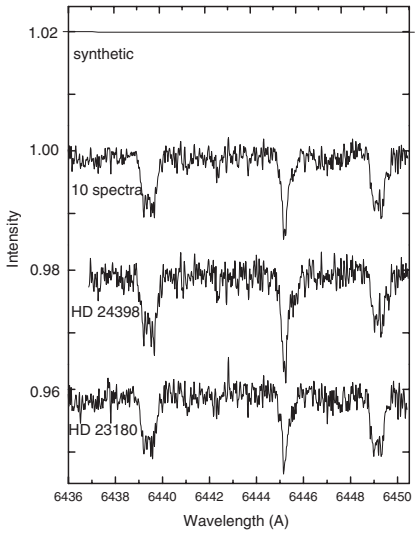

Fig. 10. The different profiles of the 6439.41, 6445.53 and 6449.16 diffuse bands – no stellar lines in this range.

widths (*EW*) and full widths at half the maximum (*FWHM*) of presented DIBs. The calculations were made by DECH procedures, which estimate the equivalent width errors depending on the *S/N* ratio in the vicinity of a feature being measured.

Figure 5 presents the range near the 4726.33 DIB. The averages of HD 24398 and HD 23180 are composed of 5 and 7 individual spectra, respectively. The resulting spectrum of HD 179406 is composed of 2 spectra, while the spectra of HD 149757 and HD 148184 are averages of 3 individual exposures each. The average, labelled "20 spectra", was made from these spectra. It is evident that this profile is composed of two substructures whose intensity ratios vary from object to object. In HD 148184, the redward substructure seems to be very strong, but its intensity could be uncertain as the presence of emission lines makes setting the position of the continuum level difficult. The existence of the stellar lines ArII 4726.851 Å, CII 4727.410 Å, and SiIII 4730.521 Å can cause rather minor broadening and increase the depth of the feature. In Galazutdinov et al. (2001), the assymetry of this profile was assigned to a stellar CII line, but the presence of a red substructure in all the targets (especially in ζ Oph which is very fast rotator) confirms its interstellar origin. Measurements of this band are given in Table 4.

Figure 6 depicts the profile of the 4963.85 DIB. The spectra of HD 24398 and HD 23180 are averages of 4 and 6 exposures, respectively. These 10 exposures, plus one of HD 148184

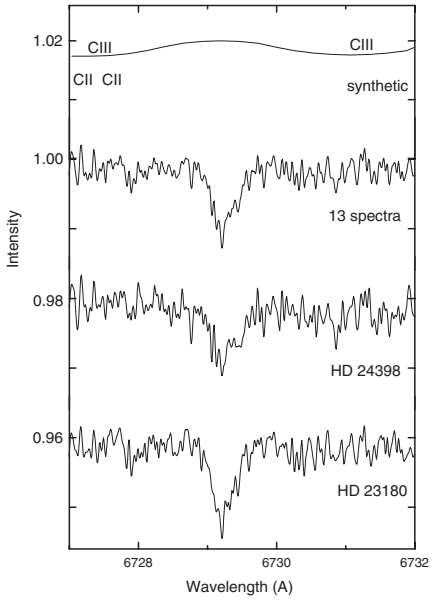

Fig. 11. The likely complex 6729.28 profile and the blending stellar lines: C II 6727.070 Å, C II 6727.260 Å, C III 6727.480 Å, and C III 6731.040 Å.

Table 4. Measurements of 4726.33 DIB. Column headings represent: DIB; HD – HD number of target star; *EW* [mÅ] – equivalent width; *EW*err [mÅ] – measuring error of *EW*; *FWHM* [Å] – full widths at half the maximum; *FWHM*err [mÅ] – measuring error of *FWHM*.

DIB	HD	*EW*	*EW*err	*FWHM*	*FWHM*err
4726.33					
	24398	60.8	7.5	3.90	0.6
	23180	64.4	4.7	3.74	0.5
	179406	68.8	4.2	2.79	0.3
	149757	38.8	2.1	3.51	0.5
	148184	162.4	3.7	3.68	0.1

Table 5. Measurements of equivalent widths *EW* [mÅ] and *FWHM* [Å] of 4963.85 DIB. Measuring errors: *EW*err [mÅ], *FWHM*err [mÅ].

DIB	HD	*EW*	*EW*err	*FWHM*	*FWHM*err
4963.85					
	24398	8.6	0.7	0.60	0.1
	23180	14.9	1.1	0.59	0.1
	148184	19.3	2.3	0.54	0.3
	149757	7.8	1.5	0.64	0.5

Table 6. Measurements of 5418.89 DIB: *EW* [mÅ] – equivalent widths, *FWHM* [Å] – full widths at half the maximum. Measuring errors: *EW*err [mÅ], *FWHM*err [mÅ].

DIB	HD	*EW*	*EW*err	*FWHM*	*FWHM*err
5418.89					
	24398	7.9	0.8	0.85	0.3
	23180	8.4	0.9	0.73	0.2

Table 7. Measurements of 5541.74, 5544.95, 5546.46 DIBs. *EW* [mÅ] – equivalent width; *EW*err [mÅ] – measuring error of *EW*; *FWHM* [Å] – full widths at half the maximum; *FWHM*err [mÅ] – measuring error of *FWHM*.

DIB	HD	*EW*	*EW*err	*FWHM*	*FWHM*err
5541.74					
	24398	4.9	0.7	0.53	0.3
	23180	6.1	0.6	0.61	0.2
5544.95					
	24398	8.6	0.7	0.74	0.1
	23180	9.2	0.7	0.73	0.1
5546.46					
	24398	3.2	0.6	0.53	0.4
	23180	5.1	0.4	0.48	0.2

and two spectra of HD 149757, were used to calculate the general average labelled "13 spectra". It is noticeable that the blue wing of the DIB is steeper than the red one, an asymmetry that clearly resembles the one demonstrated in Galazutdinov et al. (2001). The profile of this feature seems, however, not to be identical in all the observed targets. The spectrum of HD 149757, plotted at the bottom, was acquired at ESO (R = 220 000) and was already presented by Galazutdinov et al. (2002b). Such high resolution enables tracing of two substructures in the flat bottom of the 4963.85 band. The presence of the substructures is seen in the spectrum of HD 148184, but a larger number of spectra is necessary to confirm their reality. Some similarity between profiles of HD 24398 and HD 149757(ESO) can be seen. However, the substructures are not clearly detectable in the R = 120 000 resolution. The red wing of the DIB profile can be slightly modified by the CII 4964.736 Å and ArII 4965.079 Å stellar lines, which should, however, hardly be noticeable in the rapidly rotating HD 149757 star.

Another weak feature, which is strong enough to allow an analysis of its profile, however, is the DIB at 5418.89 Å. Figure 7 shows its asymmetrical profile and possibly a flat core. Averages of individual stars, HD 24398 and HD 23180, are made out of 7 and 8 spectra, respectively. Their shapes look different, which may suggest a high sensitivity of this band carrier to the varying physical conditions in the intervening clouds. It is difficult to decide whether the profile can be composed of some substructures. No stellar features have been identified in its close vicinity. In both target stars the profile has similar widths (Table 6).

A characteristic "triplet" of DIBs is situated at 5541.74, 5544.95 and 5546.46 Å. Their vicinity, as depicted in Fig. 8, contains SiIII 5539.926 Å, NII 5540.061 Å, and NII 5543.471 Å, all weak stellar lines that can contaminate them. The average of HD 24398 is made out of four spectra, and for HD 23180 of six spectra. The depicted profiles are clearly asymmetrical. The 5544.95 profile suggests the presence of two substructures, the blue one being stronger. The very weak stellar lines shown in the synthetic spectrum cannot contaminate this profile. In the case of 5541.74 DIB, the stellar contamination can broaden it. The 5546.46 profile is not very contaminated, but its individual profiles in front of different stars may be different: it has a flat core in the average of HD 23180 where it is the strongest, whilst it is nearly triangle-shaped in HD 24398 where it is much weaker (Table 7).

Table 8. Measurements of 5762.73, 5766.05, 5769.09 DIBs. *EW* [mÅ]; *EW*err [mÅ] – measuring error of *EW*; *FWHM* [Å]; *FWHM*err [mÅ] – measuring error of *FWHM*.

DIB	HD	*EW*	*EW*err	*FWHM*	*FWHM*err
5762.73					
	24398	5.1	0.5	0.63	0.2
	23180	5.1	0.6	0.50	0.2
	179406	6.6	0.9	0.58	0.3
	148184	–	–	–	–
5766.05					
	24398	3.6	0.5	0.58	0.3
	23180	5.7	0.8	0.64	0.4
	179406	11.9	1.8	1.03	0.5
	148184	5.4	0.8	0.69	0.5
5769.09					
	24398	2.9	0.4	0.44	0.4
	23180	5.1	0.5	0.47	0.2
	179406	8.2	1.0	0.49	0.2
	148184	8.8	1.0	0.74	0.2

Another "triplet" of weak diffuse bands is situated a bit bluewards of the major 5780 DIB. The weak features are situated approximately at 5762.73, 5766.05, and 5769.09 Å. Figure 9 presents the spectra of HD 24398, HD 23180 composed of 6 spectra each, and also HD 179406 and HD 148184 composed of 2 and 3 individual exposures, respectively. The profile of 5762.73 band is asymmetric and seems to contain two partially resolved substructures. In HD 179406, the DIB is the strongest, whilst in HD 148184 it is hardly detectable (Table 8). The band does not seem to be seriously contaminated with stellar lines. The presence of NeI 5764.419 Å hardly influences it, because it is too weak. The 5766.05 DIB is evidently asymmetric, with the blue wing steeper. Its red wing is likely to be contaminated with the stellar atomic line NII 5767.446 Å. The latter can also slightly modify the 5769.09 diffuse band – the DIB of an apparently featureless profile. Its intensity seems significantly different from the analysed objects. The same spectra taken together form the general average, which is also shown.

At 6439.41, 6445.53, and 6449.16 Å, one can observe another "triplet" of weak interstellar features. Figure 10 presents their profiles as apparently differing in width and shape: the 6439.41 is most likely composed of two features that are comparable in strength and shape, which makes the band symmetrical. The profile of the 6445.53 is evidently narrower than the former and is evidently asymmetric. The width of the 6449.16 band is similar to that of 6439.41; the band may suggest some internal structure, but a higher resolution seems necessary to resolve it. The spectrum of HD 23180 contains six – HD 24398 four – individual exposures. There are no stellar lines in any close vicinity of these bands, according to the synthetic spectra. For detailed measurements of these DIBs, see Table 9.

Another weak DIB of apparently complex profile is the 6729.28 one, depicted in Fig. 11. The individual profiles in HD 24398 and HD 23180 contain six and seven spectra, respectively. The general average made out of these spectra (labelled "13 spectra") may suggest that the evidently asymmetric band profile contains two or three substructures. Within the band's spectral range four stellar lines: CII 6727.070 Å, CII 6727.260 Å, CIII 6727.480 Å, CIII 6731.040 Å can be traced. They are, however, very weak and not centred close to the band's core, which makes the contamination rather unlikely.

Table 9. Measurements of *EW* [mÅ] and *FWHM* [Å] of 6439.41, 6445.53, 6449.16 DIBs. Measuring errors: *EW*err [mÅ], *FWHM*err [mÅ].

DIB	HD	*EW*	*EW*err	*FWHM*	*FWHM*err
6439.41					
	24398	7.2	0.8	0.71	0.2
	23180	7.1	0.9	0.72	0.2
6445.53					
	24398	6.7	0.8	0.34	0.1
	23180	5.2	0.6	0.48	0.1
6449.16					
	24398	5.7	0.7	0.66	0.3
	23180	6.5	0.7	0.68	0.2

Table 10. Measurements of 6729.28 DIB. *EW* [mÅ] – equivalent width; *EW*err [mÅ] – measuring error of *EW*; *FWHM* [Å] – full widths at half the maximum; *FWHM*err [mÅ] – measuring error of *FWHM*.

DIB	HD	*EW*	*EW*err	*FWHM*	*FWHM*err
6729.28					
	24398	3.4	0.6	0.49	0.3
	23180	4.6	0.5	0.40	0.1

4. Conclusions

Some previously published, high-resolution profiles of strong DIBs show complex profiles that suggest a molecular pattern (Sarre et al. 1995; Kerr et al. 1998). This fact supports the hypothesis of some complex molecular species as their carriers. The recent paper by Galazutdinov et al. (2002b) proves that some weak interstellar features also have complex profiles, which in turn may strongly suggest that they generally have the same origin as the strong ones.

This paper extends the list of weak DIBs, in which one can also trace some internal structure. Although we studied only selected weak features for which we obtained a high enough *S/N* ratio, it is suggestive that all, both strong and weak DIBs, may share a similar origin, most likely a molecular one. This is, however, more likely the case since laboratory spectra of linear hydrocarbons usually contain one strong feature and a couple of weak ones each. Spectra of high resolution and a high *S/N* are necessary to draw such a conclusion. The presented spectra of resolution $R = 120\,000$ and signal-to-noise ratio of ~300–~500 for individual stars and ~800–~1200 for averages of several stars are sufficient to suggest a complex structure of several weak DIBs. However, their strengths cannot be measured with great precision, and it is impossible to state that they correlate with other interstellar features. A more detailed analysis of the profile details of weak DIBs clearly requires a higher resolution, most likely about $R = 200\,000$.

The possible contamination by stellar lines is a serious problem while analysing DIB profiles, especially the weak ones. This effect is not important in the spectra of fast rotators (such as ζ Oph), but in slowly rotating stars (like supergiants) some of the profiles may be seriously contaminated. We examined the influence of stellar lines using a synthetic spectrum that allows the most reliable identification of all contaminating lines. Most of the depicted profiles are clearly asymmetric, and substructures can be traced inside the strongest ones. The pattern of these substructures can differ from one target to another. The equivalent widths of certain features can change considerably (e.g. 4963.85), whilst measurements of other bands remain similar (e.g. 5762.73). In this respect the behaviour of analysed weak diffuse bands clearly resembles that of strong DIBs (see Galazutdinov et al. 2002a). The variations in profiles may correspond to the physical conditions of the interstellar clouds. Hence, comparison of DIBs with laboratory counterparts remains difficult. A much broader survey of high resolution and high *S/N* ratio DIB profiles is clearly necessary to collect the data to allow a direct comparison between astrophysical observations and gas-phase experimental spectra of the suspect molecules.

Acknowledgements. The authors acknowledge the financial support of the Polish State Committee for Scientific Research (grant 2P03D 019 23). They are also very grateful to the Terskol Observatory staff members for their support during the observations. We thank Boud Roukema for a careful reading of the manuscript. G.A.G. is grateful to the Korean MOST (Ministry of Science and Technology) (grant M1-022-00-0005) and KOSFT for providing an opportunity to work at KAO through the Brain Pool program. G.A.G. and F.A.M. also want to express their thanks to the Russian Foundation for Basic Research (under grant No. 02-02-17423) and the Federal program "Astronomy" for financial support.

References

Foing, B. H., & Ehrenfreund, P. 1995, in The Diffuse Interstellar Bands, ed. A. G. G. M. Tielens, & T. P. Snow (Kluwer Academic Publ.), 65
Galazutdinov, G. A. 1992, Prep. Spets. Astrof. Obs., No. 92
Galazutdinov, G. A., Musaev, F. A., Krełowski, J., & Walker, G. A. H. 2000, Publs. Astr. Soc. Pacific, 112, 648
Galazutdinov, G. A., Musaev, F. A., Schmidt, M. R., & Krełowski, J. 2001, MNRAS, 323, 293
Galazutdinov, G. A., Moutou, C., Musaev, F. A., & Krełowski, J. 2002a, A&A, 384, 215
Galazutdinov, G. A., Stachowska, W., Musaev, F. A., et al. 2002b, A&A, 396, 987
Gies, D. R., & Lambert, D. L. 1992, ApJ, 387, 673
Heber, U. 1983, A&A, 118, 39
Heger, M. L. 1921, Lick Obs. Bull., 10, 141
Herbig, G. H. 1975, ApJ, 196, 129
Herbig, G. H., & Soderblom, D. R. 1982, ApJ, 252, 610
Hubeny, I., Harmanec, P., & Stefl, S. 1986, Bull. Astron. Inst. Czech., 37, 370
Hubeny, I., Lanz, T., & Jeffery, C. S. 1995, SYNSPEC–A user's Guide, version 36, CCP7 Electron. Libr.
Kerr, T. H., Hibbins, R. E., Fossey, S. J., Miles, J. R., & Sarre, P. J. 1998, ApJ, 495, 941
Krełowski, J., & Walker, G. A. H. 1987, ApJ, 312, 860
Krełowski, J., & Schmidt, M. R. 1997, ApJ, 484, 720
Krełowski, J., Galazutdinov, G. A., & Musaev, F. A. 1998, ApJ, 493, 217
Krełowski, J., Ehrenfreund, P., Foing, B. H., et al. 1999, A&A, 347, 235
Kurucz, R. L. 1992, in ed. B. Barbuy, & A. Renzini, The Stellar Populations of Galaxies (Dordrecht: Kluwer), Proc. IAU Symp., 149, 225
Kurucz, R. L. 1993a, SAO Cambridge, CDROM 14
Kurucz, R. L. 1993b, SAO Cambridge, CDROM 18
Kurucz, R. L., & Bell, B. 1995, SAO Cambridge, CD-ROM No. 23
Lamers, H. J. G. L. M., & Leitherer, C. 1993, ApJ, 412, 771
Lyubimkow, L. S. 1998, Astronomy Rep., 42, 312
Martin, W. C., Fuhr, J. R., Kelleher, D. E., et al. 1999, NIST Atomic Spectra Database, (version 2.0), (Online), available: `http://physics.nist.gov/asd` (April, 2004), National Institute of Standards and Technology, Gaithersburg, MD
McErlean, N. D., Lennon, D. J., & Dufton, P. L. 1999, A&A, 349, 553
Merrill, P. W., Sanford, R. F., Wilson, O. C., & Burwell, C. G. 1937, ApJ, 86, 274
Motylewski, T., Linnartz, H., Vaizert, O., & Maier, J. P. 2000, ApJ, 531, 312
Musaev, F. A., Galazutdinov, G. A., Sergeev, A. V., et al. 1999, Kinematika i Fizika Nebesnyh Tel, 15(3)
Piskunov, N. E., Kupka, F., Ryabchikova, T. A., Weiss, W. W., & Jeffrey, C. S. 1995, A&AS, 112, 525
Ruiterkamp, R., Halasinski, T., Salama, F., et al. 2002, A&A, 390, 1153
Salama, F., Galazutdinov, G. A., Krełowski, J., Allamandola, L. J., & Musaev, F. A. 1999, ApJ, 526, 265
Sarre, P. J., Miles, J. R., Kerr, T. H., et al. 1995, MNRAS, 277, 41
Schulz, S. A., King, J. E., & Glinski, R. J. 2000, MNRAS, 312, 769
Snow, T. P. 2002, ApJ, 567, 407
Thorburn, J. A., Hobbs, L. M., McCall, B. J., et al. 2003, ApJ, 584, 339
Underhill, A. B., Divan, L., Prévot-Burnichon, M. L., & Doazan, V. 1979, MNRAS, 189, 601
Walker, G. A. H., Bohlender, D. A., & Krełowski, J. 2000, ApJ, 530, 362
Welty, D. E., & Hobbs, L. M. 2001, ApJS, 133, 345
Westerlund, B., & Krełowski, J. 1988, A&A, 203, 134